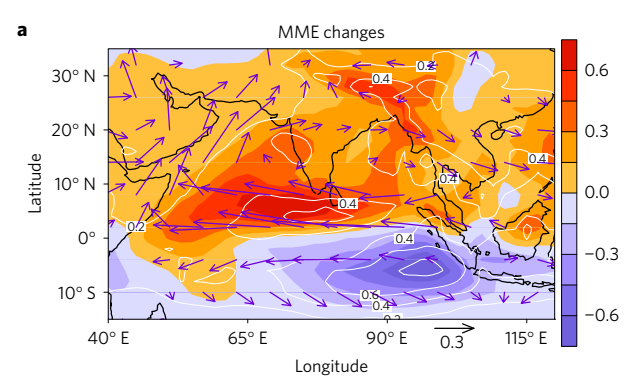
Western Pacific emergent constraint lowers projected increase in Indian summer monsoon rainfall

Gen Li^{1*}, Shang-Ping Xie^{2,3}, Chao He⁴ and Zesheng Chen¹

The agrarian-based socioeconomic livelihood of densely populated South Asian countries is vulnerable to modest changes in Indian summer monsoon (ISM) rainfall¹⁻³. How the ISM rainfall will evolve is a question of broad scientific and socioeconomic importance³⁻⁹. In response to increased greenhouse gas (GHG) forcing, climate models commonly project an increase in ISM rainfall⁴⁻⁹. This wetter ISM projection, however, does not consider large model errors in both the mean state and ocean warming pattern⁹⁻¹¹. Here we identify a relationship between biases in simulated present climate and future ISM projections in a multi-model ensemble: models with excessive present-day precipitation over the tropical western Pacific tend to project a larger increase in ISM rainfall under GHG forcing because of too strong a negative cloud-radiation feedback on sea surface temperature. The excessive negative feedback suppresses the local ocean surface warming, strengthening ISM rainfall projections via atmospheric circulation. We calibrate the ISM rainfall projections using this 'present-future relationship' and observed western Pacific precipitation. The correction reduces by about 50% of the projected rainfall increase over the broad ISM region. Our study identifies an improved simulation of western Pacific convection as a priority for reliable ISM projections.

The ISM is an important component of the global climate system¹²⁻¹⁹, and provides a large proportion (up to 80%) of annual precipitation for densely populated countries such as India^{20,21}. Slight changes in ISM rainfall could exert tremendous socioeconomic impacts throughout South Asia^{1-3,20,21}, including agriculture, ecosystems, water resources, economies, and health. For example, a 19% decrease in the ISM rainfall during 2002 caused economic damages on the order of billions of dollars²² and affected the lives of more than one billion people. Thus, determining the response of regional ISM rainfall to global warming is important for adaptation to climate change.

The Intergovernmental Panel on Climate Change (IPCC) Fifth Assessment Report (AR5) concluded that climate models robustly project an increase in ISM rainfall under greenhouse warming and the projected ISM rainfall change increases with anthropogenic forcing⁴. This result relies heavily on climate model projections, as the monsoon rainfall change due to greenhouse warming is difficult to detect from instrumental records against a backdrop of large natural variability^{4,6,19}. Climate models, however, commonly suffer from serious systematic biases in present climate simulations (such as excessive precipitation over the tropical western Pacific)^{10,11},



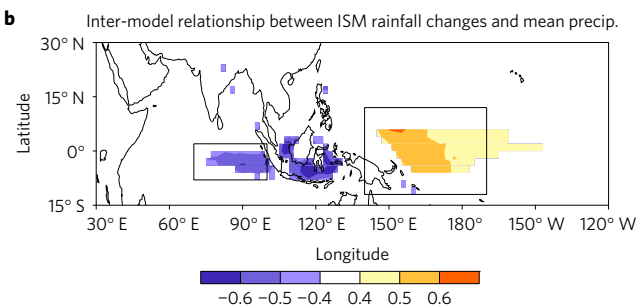


Figure 1 | Regional climate changes during the ISM season (May to September) and the relationship between ISM rainfall changes and mean precipitation. a, The MME mean changes in rainfall (colour shade, mm d $^{-1}$) and 850-hPa wind (vector scale is shown in the lower right corner, m s $^{-1}$) from 1980-2009 to 2070-2099 projected by 24 CMIP5 models under the RCP 8.5 scenario. In a, the white contours display the inter-model standard deviations of rainfall changes. b, Inter-model correlations between the inter-model spreads in projected rainfall change averaged over the ISM region (60°-95° E, 10°-30° N) and in simulated present-day precipitation over the Indo-Pacific. In b, solid boxes denote the tropical western Pacific (140° E-170° W, 12° S-12° N) and southeastern Indian Ocean (SEIO; 70°-100° E, 8° S-2° N) and colour shading indicates regions of significance at the 95% level according to t-test. All the climatology changes in this study are normalized by the corresponding global mean SST increase for each model, unless otherwise specified.

potentially reducing the reliability of future projections. Here we show that the excessive precipitation bias in the present-day simulation over the tropical western Pacific exaggerates the response

¹State Key Laboratory of Tropical Oceanography, South China Sea Institute of Oceanology, Chinese Academy of Sciences, Guangzhou, Guangdong 510301, China. ²Scripps Institution of Oceanography, University of California San Diego, La Jolla, California 92093-0206, USA. ³Physical Oceanography Laboratory/CIMST, Ocean University of China, and Qingdao National Laboratory for Marine Science and Technology, Qingdao, Shandong 266100, China. ⁴Institute of Tropical and Marine Meteorology (ITMM), China Meteorological Administration (CMA), Guangzhou, Guangdong 510640, China. ^{*}e-mail: ligen@scsio.ac.cn

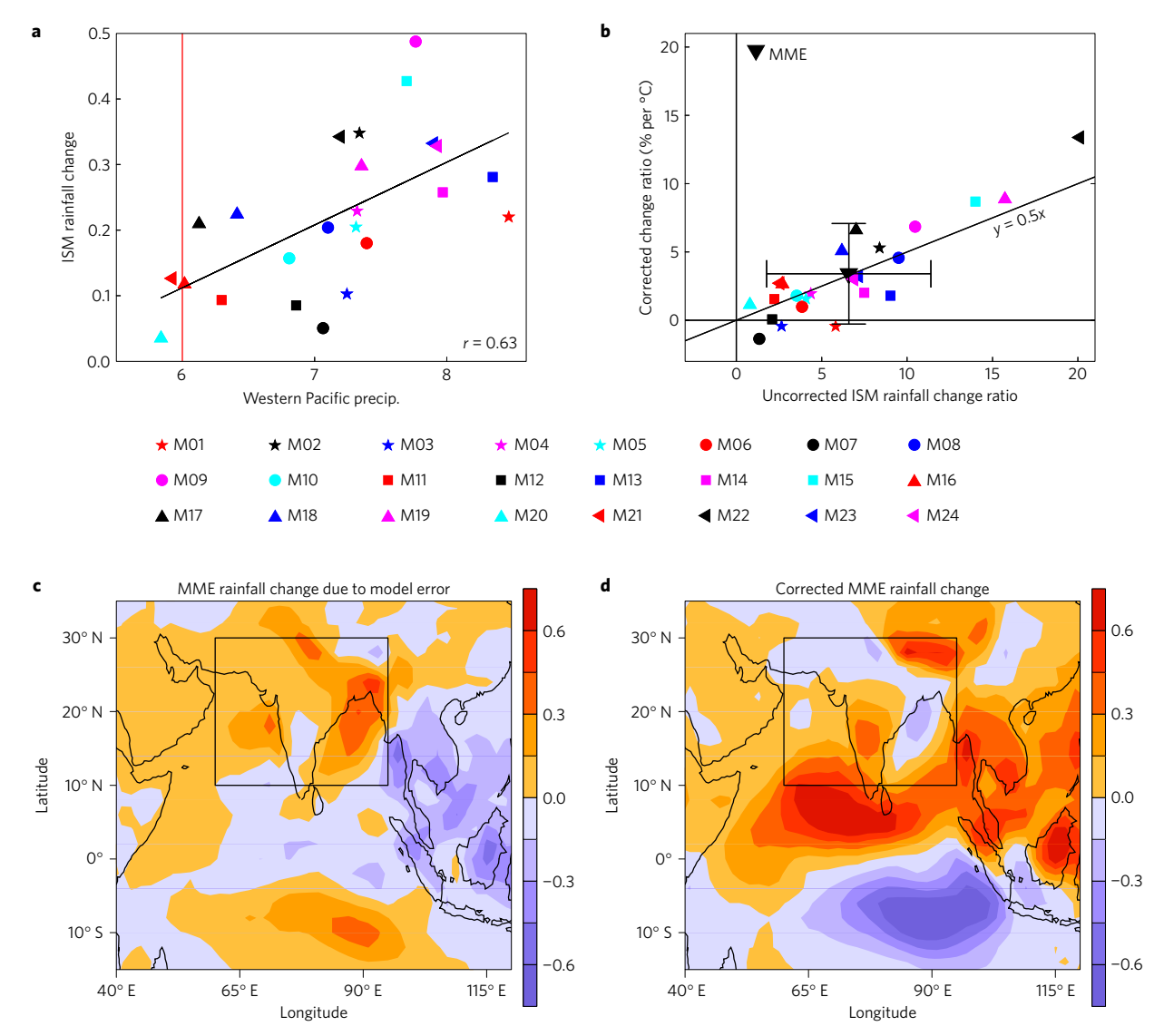


Figure 2 | Inter-model relationship between the present-day simulations and future projections and corrections of regional climate projections. \mathbf{a} , \mathbf{b} , Scatterplots of the simulated tropical western Pacific precipitation (mm d⁻¹) versus projected average ISM rainfall changes under the RCP 8.5 scenario (\mathbf{a}) and the uncorrected versus corrected average ISM rainfall change ratios (% per degree Celsius of global SST warming) (\mathbf{b}) for 24 CMIP5 models and their MME mean. In \mathbf{a} , the red line denotes the observed present-day western Pacific precipitation and the inter-model correlation (r) is shown in the lower right corner. In \mathbf{b} , the error bars for the MME means indicate the standard deviation spread among models and the 2:1 line ('y = 0.5x') is used to illustrate the MME mean reduction in projected rainfall increase. \mathbf{c} , The MME mean errors of projected precipitation changes as evaluated from the simulated tropical western Pacific biases. \mathbf{d} , Same as \mathbf{c} , but for corrected MME mean changes. In \mathbf{c} and \mathbf{d} , the boxes are used to define average ISM rainfall.

of ISM rainfall to GHG forcing by affecting the tropical Pacific sea surface temperature (SST) warming pattern and adjacent monsoon circulation. The projected ISM rainfall increase and inter-model uncertainty under increased GHG forcing are both greatly scaled down after the corrections with the observed western Pacific precipitation.

The historical simulations and Representative Concentration Pathway (RCP) 8.5 experiments from 24 CMIP5 models (see Methods and Supplementary Table 1) are used to represent the present and future climates, respectively 23 . Figure 1a shows the multi-model ensemble (MME) mean changes in precipitation and 850-hPa wind during the ISM season. Consistent with previous studies $^{4-9}$, the projected change in ISM rainfall features a spatially coherent wet trend with a maximum extending from the Bay of Bengal to the north-eastern Indian subcontinent. All models consistently project an increase for ISM rainfall, at $\sim\!6.5\%$ per degree Celsius of global SST warming in the MME mean (Fig. 2b).

The change in 850-hPa wind shows pronounced easterly (westerly) anomalies south (north) of \sim 15° N (Fig. 1a), which weakens

the Webster–Yang index (WYI¹², a widely used ISM circulation index; Supplementary Fig. 1). Based on the monsoon meridional circulation index (MMCI)¹³, however, greenhouse warming intensifies the meridional circulation north of 10° N with increased atmospheric moisture²⁴ over the ISM region of increased rainfall (Supplementary Fig. 1). Large inter-model uncertainty in ISM rainfall changes mainly results from that in changes in atmospheric circulation rather than moisture (Supplementary Fig. 2).

Recent studies^{9,25} suggested that inter-model difference in SST warming over the tropical western Pacific is a dominant source of uncertainty in projected changes in Asian–Australian monsoon circulation/rainfall. In particular, both the multi-model statistics and modelling experiments show that the inter-model spread in ISM circulation/rainfall projections is highly correlated with the tropical western Pacific SST warming⁹. On the other hand, the western Pacific SST warming is strongly dampened by a negative cloud–radiation feedback²⁶ that depends on the local mean cloud/precipitation amount¹⁰. Cloudy/rainy models in the western

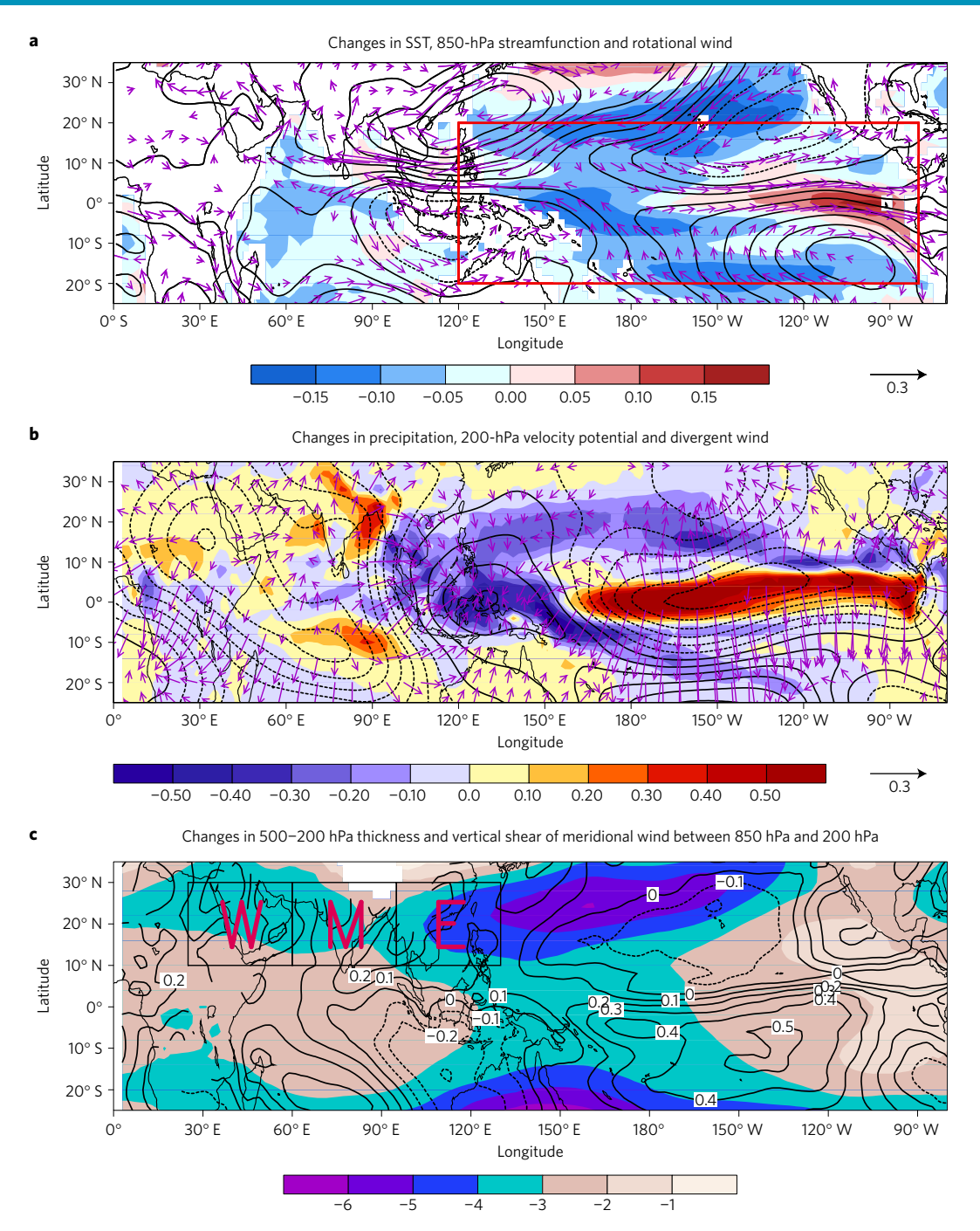


Figure 3 | Inter-model regressions of projected changes under the RCP 8.5 scenario against the simulated present-day precipitation (mm d^{-1}) averaged over the tropical western Pacific. **a**, Projected changes in SST (colour shaded, °C), 850-hPa streamfunction (contour interval: $0.5 \times 10^5 \text{ s}^{-1}$) and rotational wind (vectors, m s⁻¹). **b**, Projected changes in precipitation (colour shaded, mm d^{-1}), 200-hPa velocity potential (contour interval: $0.5 \times 10^5 \text{ m}^2 \text{ s}^{-1}$) and divergent wind (vectors, m s⁻¹). **c**, Projected changes in 500-200 hPa thickness (colour shaded, m) and vertical shear of meridional wind (contours, m s⁻¹) between 850 hPa and 200 hPa. In **a**, the red box shows the tropical Pacific region (120° E-80° W, 20° S-20° N) where the SST anomalies are used to force the sensitivity experiment (see Methods). In **c**, the 500-200 hPa thickness difference between boxes E and W denotes zonal gradient of middle-upper tropospheric temperature across the ISM region and the weakened zonal temperature gradient between boxes E and W is accompanied by a strengthened vertical shear of meridional wind between 850 hPa and 200 hPa in box M.

Pacific have a stronger cloud–radiation feedback that dampens the local SST warming. Indeed, the inter-model spread in ISM rainfall changes is significantly correlated with that in simulated present-day precipitation over the tropical western Pacific and southeastern Indian Ocean (SEIO; Fig. 1b). Similar results are obtained from the CMIP3 ensemble (see Methods and Supplementary Fig. 3).

Figure 3 explores how projected changes are related to the biases in simulating present-day precipitation over the tropical western

Pacific. Models with excessive present-day precipitation there tend to project a weaker local SST warming and a stronger warming in the equatorial eastern Pacific (Fig. 3a and Supplementary Fig. 4). This is because models with more mean precipitation over the tropical western Pacific tend to feature a larger increase in local precipitation per degree SST increase on interannual timescales, and models with a stronger interannual precipitation sensitivity there tend to have a greater reduction in downwelling surface shortwave (SW)

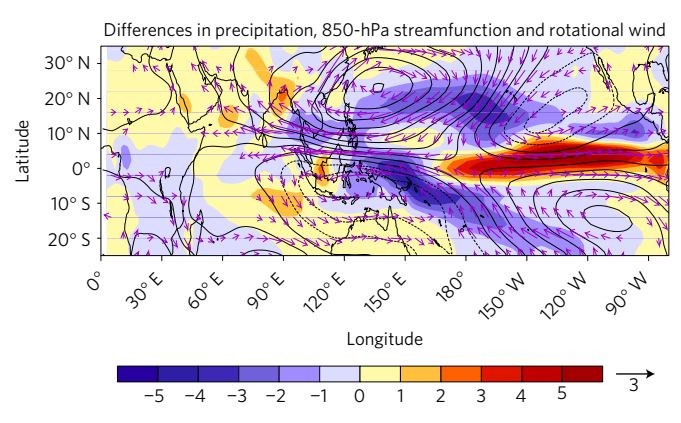


Figure 4 | Atmospheric response to the tropical Pacific warming pattern related to the tropical western Pacific precipitation biases in the CAM4 experiment. Exp_SE minus Exp_CNTL differences (see Methods) in precipitation (colour shaded, mm d $^{-1}$), 850-hPa streamfunction (contour interval: $5 \times 10^5 \, \mathrm{s}^{-1}$) and rotational wind (vectors, m s $^{-1}$) during the ISM season. Here, the tropical Pacific SST anomalies used to force the sensitivity experiment are those included in the red box of Fig. 3a, except for a ten-time magnitude of the pattern to increase the signal-to-noise ratio.

radiation with local SST increase both on interannual timescales and in climate change, dampening local SST warming and resulting in an enhanced east-minus-west gradient of Pacific SST warming (Supplementary Fig. 5). Reduced SST warming over the western Pacific is associated with a Gill-type Rossby circulation response^{14,27,28}: low-level anticyclone anomalies in the Indian Ocean and Asian continent weaken zonal wind south of ~15° N but strengthen the ISM meridional circulation. Southerly anomalies on the western flank of this anomalous anticyclone transport ocean moisture into the Indian subcontinent (Fig. 3a), increasing ISM convection and rainfall (Fig. 3b). Such a Rossby-wave response is also evident in middle-upper tropospheric temperature. Due to reduced SST warming (Fig. 3a) and suppressed convective heating (Fig. 3b) over the western Pacific, tropospheric temperature is cooled over Southeast Asia (Fig. 3c and Supplementary Fig. 4). The resultant zonal temperature gradient anomalies across the ISM region act to enhance the vertical shear of meridional wind, monsoon ascending motion, and rainfall (Fig. 3c and Supplementary Figs 6 and 7).

To corroborate the effect of the Pacific SST warming bias pattern on ISM change in warmer climate, we perform an experiment using the Community Atmosphere Model version 4 (CAM4; see Methods). With the tropical Pacific SST warming pattern (as shown in the red box of Fig. 3a) related to the western Pacific precipitation biases, the model reproduces the Gill-type Rossby circulation response and resultant ISM rainfall anomalies (Fig. 4), consistent with the CMIP5 multi-model analysis (Fig. 3). This confirms the role of the Pacific SST warming in ISM change.

Therefore, errors in present-day precipitation simulation over the tropical western Pacific could cause biases in projected ISM rainfall change by influencing the Pacific SST warming pattern. The same relationship holds in the CMIP3 ensemble (Supplementary Fig. 3). CMIP5 models with excessive western Pacific precipitation tend to project a larger increase in ISM rainfall under global warming, with a high inter-model correlation of 0.63 at the 99.9% significance level according to t-test (Fig. 2a). Thus, the western Pacific precipitation biases explain around 40% of inter-model uncertainty in ISM rainfall projections. This offers an 'observational constraint' to correct ISM rainfall projections (see Methods). Our correction based on the multi-model relationship between an observable quantity (present-day western Pacific precipitation) and future ISM projections is similar to the 'emergent constraint' concept^{29,30}. For emergent constraints, it is important to evaluate

whether the identified 'present-future' relationship is physical. The relationship between western Pacific precipitation biases in the mean and projected ISM rainfall changes is not only statistically significant but also consistent with our understanding of negative cloud-radiation feedback²⁶ in the western Pacific and the Gill-type Rossby circulation response²⁷ that affects the ISM. Thus, this 'present-future' relationship appears physically credible.

The MME errors in projected change as evaluated from the present-day western Pacific precipitation biases feature a broad increase in ISM rainfall, especially from the Bay of Bengal to the northeastern Indian subcontinent (Fig. 2c). By calibrating each model against the observed western Pacific precipitation, the corrected projection no longer shows spatially coherent increases for ISM rainfall under greenhouse warming (Fig. 2d). The corrected change in ISM rainfall drops from \sim 6.5% to \sim 3.5% per degree Celsius of global SST warming in the MME mean, and even becomes negative in a few models (Fig. 2b). The inter-model spread in corrected ISM rainfall changes is comparable to the MME mean precipitation increase, although the corrected ISM rainfall changes are constrained to a smaller range (Fig. 2b). These results cast doubts on the 'robust' projection of increased ISM rainfall in warmer climate.

The inter-model uncertainty in projected ISM rainfall changes is also significantly correlated with errors in simulating SEIO precipitation (Fig. 1b). The inter-model spread in simulated SEIO precipitation is not independent of that in tropical western Pacific precipitation (the inter-model correlation is -0.58, exceeding the 99% significance level according to t-test). Together, the wet bias in the western Pacific and dry bias in the SEIO represent the Indo-Pacific Walker circulation modulation (Supplementary Fig. 8). We can build an alternative emergent constraint based on the observed precipitation difference between the western Pacific and SEIO (see Methods). This Walker circulation index correlates with the projected ISM rainfall changes at 0.73 among 24 CMIP5 models (Supplementary Fig. 9), explaining more inter-model spread in ISM rainfall projections (>50%) than the western Pacific precipitation index. As the MME mean biases in SEIO precipitation are small (figure not shown), the physical relationship between errors in the Walker circulation index and projected ISM change is very similar to that with the western Pacific precipitation index described earlier (Supplementary Fig. 10). The pattern of the correction based on an 'observational constraint' of this Walker circulation index (Supplementary Fig. 9) is very similar to that without including SEIO precipitation biases (Fig. 2d), with the pattern correlation of 0.96. The regional average ISM rainfall changes corrected with the Walker circulation and western Pacific precipitation indices for 24 CMIP5 models are also very similar, with the inter-model correlation of 0.90 (figure not shown). All this suggests that the emergent constraints we identified here are robust and physical.

In summary, the emergent constraint of tropical western Pacific precipitation lowers the projected increase in ISM rainfall under global warming. Our results show that the common model biases of excessive precipitation over the tropical western Pacific dampen local SST warming, and thus artificially increase ISM rainfall change by enhancing the ISM meridional circulation. By adjusting western Pacific precipitation to the observed value, the projected increase in rainfall over the broad ISM region is reduced by about 50%.

The comparison of coupled and atmospheric model pairs indicates that the excessive western Pacific precipitation errors are already present in atmosphere-only models (figure not shown), and may be associated with errors in parameterizing deep convection¹⁰. Our corrections reduce the uncertainty in ISM rainfall projections by removing the linear influence of tropical western Pacific precipitation biases, but our method does not rule out the effects of other model biases. Our results point to improving the simulation of tropical western Pacific convection as an important step towards more reliable projections of ISM circulation and rainfall changes.

The benefits are enormous for more than a billion people living in the monsoon.

Methods

Methods, including statements of data availability and any associated accession codes and references, are available in the online version of this paper.

Received 18 March 2017; accepted 11 August 2017; published online 18 September 2017

References

- Gadgil, S. & Gadgil, S. The Indian monsoon, GDP and agriculture. Econ. Polit. Weekly 41, 4887–4895 (2006).
- Wahl, E. R. & Morrill, C. Toward understanding and predicting monsoon patterns. Science 328, 437–438 (2010).
- 3. Douglas, I. Climate change, flooding and food security in south Asia. *Food Secur.* **1**, 127–136 (2009).
- 4. Christensen, J. H. et al. in Climate Change 2013: The Physical Science Basis (eds Stocker, T. F. et al.) 1217–1308 (IPCC, Cambridge Univ. Press, 2014).
- Meehl, G. A. & Washington, W. M. South Asian summer monsoon variability in a model with doubled atmospheric carbon dioxide concentration. *Science* 260, 1101–1104 (1993).
- Turner, A. G. & Annamalai, H. Climate change and the South Asian summer monsoon. *Nat. Clim. Change* 2, 587–595 (2012).
- May, W. Simulated changes of the Indian summer monsoon under enhanced greenhouse gas conditions in a global time-slice experiment. *Geophys. Res. Lett.* 29, 1118 (2002).
- 8. Sooraj, K. P., Terray, P. & Mujumdar, M. Global warming and the weakening of the Asian summer monsoon circulation: assessments from the CMIP5 models. *Clim. Dynam.* **45**, 233–252 (2015).
- Chen, X. & Zhou, T. Distinct effects of global mean warming and regional sea surface warming pattern on projected uncertainty in the South Asian summer monsoon. *Geophys. Res. Lett.* 42, 9433–9439 (2015).
- Lin, J. L. The double-ITCZ problem in IPCC AR4 coupled GCMs: ocean-atmosphere feedback analysis. J. Clim. 20, 4497–4525 (2007).
- Li, G., Xie, S. P. & Du, Y. Monsoon-induced biases of climate models over the tropical Indian Ocean. J. Clim. 28, 3058–3072 (2015).
- Webster, P. J. & Yang, S. Monsoon and ENSO: selectively interactive systems. Q. J. R. Meteorol. Soc. 118, 877–926 (1992).
- Goswami, B. N., Krishnamurthy, V. & Annamalai, H. A broad-scale circulation index for the interannual variability of the Indian summer monsoon. Q. J. R. Meteorol. Soc. 125, 611–633 (1999).
- Annamalai, H., Hafner, J., Sooraj, K. P. & Pillai, P. Global warming shifts the monsoon circulation, drying South Asia. J. Clim. 26, 2701–2718 (2013).
- Kumar, K. K., Rajagopalan, B., Hoerling, M. P., Bates, G. & Cane, M. Unraveling the mystery of Indian monsoon failure during El Niño. Science 314, 115–119 (2006).
- Bollassina, M. A., Ming, Y. & Ramaswamy, V. Anthropogenic aerosols and the weakening of the South Asian summer monsoon. *Science* 224, 502–505 (2011).
- Goswami, B. N., Venugopal, V., Sengupta, D., Madhusoodanan, M.
 Xavier, P. K. Increasing trend of extreme rain events over India in a warming environment. *Science* 314, 1442–1445 (2006).

- Boos, W. R. & Kuang, Z. Dominant control of the South Asian monsoon by orographic insulation versus plateau heating. *Nature* 463, 218–222 (2010).
- Roxy, M. K. et al. Drying of Indian subcontinent by rapid Indian Ocean warming and a weakening land–sea thermal gradient. Nat. Commun. 6, 7423 (2015).
- Bollasina, M. A. Hydrology: probing the monsoon pulse. Nat. Clim. Change 4, 422–423 (2014).
- Jain, S. K. & Kumar, V. Trend analysis of rainfall and temperature data for India. Curr. Sci. 102, 37–49 (2012).
- Gadgil, S., Vinayachandran, P. N., Francis, P. A. & Gadgil, S. Extremes of the Indian summer monsoon rainfall, ENSO and equatorial Indian Ocean oscillation. *Geophys. Res. Lett.* 31, L12213 (2004).
- Taylor, K. E., Ronald, J. S. & Meehl, G. A. An overview of CMIP5 and the experiment design. *Bull. Am. Meteorol. Soc.* 93, 485–498 (2012).
- Held, I. M. & Soden, B. J. Robust responses of the hydrological cycle to global warming. J. Clim. 19, 5686–5699 (2006).
- 25. Brown, J. R., Moise, A. F., Colman, R. & Zhang, H. Will a warmer world mean a wetter or drier Australian monsoon? *J. Clim.* 29, 4577–4596 (2016).
- Meehl, G. A. & Washington, W. M. El Niño-like climate change in a model with increased atmospheric CO₂ concentrations. *Nature* 382, 56–60 (1996).
- Gill, A. E. Some simple solutions for heat-induced tropical circulation. Q. J. R. Meteorol. Soc. 106, 447–462 (1980).
- Shaman, J. & Tziperman, E. The effect of ENSO on Tibetan Plateau snow depth: a stationary wave teleconnection mechanism and implications for the South Asian monsoons. J. Clim. 18, 2067–2079 (2005).
- Boe, J. L., Hall, A. & Qu, X. September sea-ice cover in the Arctic Ocean projected to vanish by 2100. Nat. Geosci. 2, 341–343 (2009).
- Cox, P. M. et al. Sensitivity of tropical carbon to climate change constrained by carbon dioxide variability. *Nature* 494, 341–344 (2013).

Acknowledgements

We are grateful for helpful comments from L. Sun and R. Lu. This work was supported by the Natural Science Foundation of China (41521005 and 41406026), the National Basic Research Program of China (2012CB955603), the Guangdong Natural Science Funds for Distinguished Young Scholar (2015A030306008), the Youth Innovation Promotion Association CAS, and the Pearl River S&T Nova Program of Guangzhou (201506010094). S.-P.X. was supported by the US National Science Foundation (1637450). Z.C. was supported by the Open Project Program of State Key Laboratory of Tropical Oceanography (LTOZZ1603). We acknowledge the climate modelling groups for producing and making available their model output, the WCRP's Working Group on Coupled Modeling (WGCM) for organizing the CMIP5 analysis activity, the Program for Climate Model Diagnostics and Intercomparison (PCMDI) for collecting and archiving the CMIP5 multi-model data, and the Office of Science, US Department of Energy for supporting these datasets in partnership with the Global Organization for Earth System Science Portals.

Author contributions

G.L. designed the study and performed the analysis with feedback from S.-P.X. G.L. and S.-P.X. wrote the paper. C.H. and Z.C. carried out the CAM4 experiments.

Additional information

Supplementary information is available in the online version of the paper. Reprints and permissions information is available online at www.nature.com/reprints. Publisher's note: Springer Nature remains neutral with regard to jurisdictional claims in published maps and institutional affiliations. Correspondence and requests for materials should be addressed to G.L.

Competing financial interests

The authors declare no competing financial interests.

Methods

Models and dataset. We examine the historical simulations and Representative Concentration Pathway (RCP) 8.5 experiments from 24 coupled general circulation models (CGCMs) participating in the Coupled Model Intercomparison Project phase 5 (CMIP5)23. The model names, modelling groups (or centres), and their letter labels are shown in Supplementary Table 1. Further information on individual models is available online at http://cmip-pcmdi.llnl.gov/cmip5/ availability.html. Precipitation, sea surface temperature (SST), downwelling surface shortwave (SW) flux, vertically integrated water vapour (Q) through the atmospheric column, 500-hPa vertical pressure velocity (ω), zonal and meridional winds at 850 hPa and 200 hPa, and geopotential height at 500 hPa and 200 hPa are used. Note that the upward velocity is positive for ω in this study, unless otherwise specified. We use the 1980-2009 mean in historical simulations as the present climatology, and the 2070-2099 mean in RCP 8.5 experiments as the future climatology. Their difference represents climate change under global warming. To eliminate the effect of inter-model difference in climate response sensitivity to greenhouse gas (GHG) forcing, all the climatology changes in this study are normalized by the corresponding global mean SST increase for each model. The multi-model ensemble (MME) mean is defined as the simple average of 24 CGCMs. To validate the CMIP5 results, Supplementary Fig. 3 also examines the Twentieth Century (20C3M) simulations and Special Report on Emissions Scenarios (SRES) A1B forcing from 21 CMIP3 models, who are CGCM3.1-T47, CGCM3.1-T63, CNRM-CM3, CSIRO-Mk3.0, CSIRO-Mk3.5, GFDL-CM2.0, GFDL-CM2.1, GISS-AOM, GISS-EH, FGOALS-g1.0, INM-CM3.0, IPSL-CM4, MIROC3.2-hires, MIROC3.2-medres, ECHO-G, ECHAM5, MRI-CGCM2.3.2, CCSM3, PCM, UKMO-HadCM3, and UKMO-HadGEM1. For observations, we use the precipitation climatology from the Global Precipitation Climatology Project (GPCP)³¹ for 1980–2009. A common 2° × 2° horizontal grid interpolation is applied to all the model outputs and observations.

Definition of monsoon indices. The South Asian region (60°-95° E, 10°-30° N) is used to define average Indian summer monsoon (ISM) rainfall. Here, the ISM season is from May to September. The present results are not sensitive to the exclusion of May from or the incorporation of October into the ISM season. Webster-Yang index (WYI)12 is defined as zonal wind difference between 850 hPa and 200 hPa averaged over the region (40°-110° E, 0°-20° N). Monsoon meridional circulation index (MMCI)¹³ is defined as the meridional wind difference between 850 hPa and 200 hPa averaged over the ISM region. The WYI satisfactorily reflects the monsoon circulation south of 20° N, in particular for the upper level³². Under greenhouse gas (GHG) forcing, the ISM circulation will be projected to feature a poleward shift^{6,33} by climate models, leading to a weakening of zonal wind south of 15° N (Fig. 1a). Thus, this ISM poleward shift will weaken the WYI (Supplementary Fig. 1). The MMCI satisfactorily reflects the ISM meridional overturning circulation north of 10° N and is closely linked to the convective heating of ISM13. Models tend to project strengthened MMCI under GHG forcing (Supplementary Fig. 1).

Sensitivity experiment. We perform a sensitivity experiment using the Community Atmosphere Model version 4 (CAM4)34 developed by the National Center for Atmospheric Research (NCAR). First, we prepare three types of SST fields: SST0, SST1 and SST2. SST0 is the monthly global climatological SST derived from observations (1979–2008)³⁵. SST1 is the projected monthly SST changes over the tropics (20° S-20° N) in the MME mean under the RCP 8.5 scenario. SST1 outside the tropics is set to zero. SST2 is the SST warming bias pattern over the tropical Pacific (120° E-80° W, 20° S-20° N) related to the tropical western Pacific precipitation biases. SST2 is shown in the red box of Fig. 3a except for a ten-time magnitude of the pattern to increase the signal-to-noise ratio, and set to zero outside the tropical Pacific. Two Atmospheric Model Intercomparison Project (AMIP)-type experiments are performed: Exp_CNTL, a control run forced by (SST0 + SST1), and Exp_SE, a sensitivity run forced by (SST0 + SST1 + SST2). We run the experiments for 30 years and the average of the last 20 years is analysed. The differences between the Exp_SE and Exp_CNTL in Fig. 4 represent the atmospheric circulation and precipitation responses to the tropical Pacific SST warming pattern related to the western Pacific precipitation biases in warmer climate. The Gill-type Rossby circulation response and the pattern of ISM rainfall anomalies from the CAM4 sensitivity experiment (Fig. 4) are very similar to the CMIP5 multi-model statistical analysis (Fig. 3). The CAM4 response is ten times larger in magnitude, consistent with the magnified SST forcing.

Correcting regional climate projections. CGCMs commonly simulate excessive present-day precipitation/cloud in the tropical western Pacific than observations^{10,36} (Fig. 2a). The precipitation bias for model *m* is expressed as:

$$P(m)' = P(m) - P_{\text{obs}} \tag{1}$$

where P(m) and $P_{\rm obs}$ represent the precipitation values in the tropical western Pacific (140° E–170° W, 12° S–12° N) for model m and observations, respectively.

The projected climate change, C(s, m), can be defined as the difference between future climatology, F(s, m), and historical climatology, H(s, m):

$$C(s,m) = F(s,m) - H(s,m)$$
(2)

where s and m denote space (latitude–longitude) and model, respectively. The 'present–future relationship' among models between the simulated western Pacific precipitation, P(m), and projected climate change, C(s,m), can be performed by a linear regression analysis as follows:

$$C(s,m) = a(s) \times P(m) + b(s) \tag{3}$$

where a is regression pattern and b is the regression constant. Where the relationship between P(m) and C(s,m) is statistically significant, the climate projection, C(s,m), can be calibrated based on this inter-model relationship and observed western Pacific precipitation, $P_{\rm obs}$, in analogy to the concept called 'emergent constraints' ^{29,30,37–40}.

Because the relationship between the simulated western Pacific precipitation and projected ISM rainfall changes in Fig. 2a is statistically significant (the inter-model correlation is 0.63, explaining around 40% of inter-model uncertainty in ISM rainfall projections) and also consistent with our understanding of negative cloud–radiation feedback²⁶ in the western Pacific and the Gill-type Rossby circulation response mechanism²⁷ as explained in the main text, we can estimate the errors of climate projection, C(s,m)', from the western Pacific precipitation bias for each model:

$$C(s,m)' = a(s) \times P(m)' \tag{4}$$

Therefore, the corrected climate changes for each model are given as:

$$C(s,m)^* = C(s,m) - C(s,m)'$$
 (5)

Finally, the MME mean of corrected future climate changes in individual models is calculated as:

$$\overline{C(s,m)}^* = \frac{1}{N} \sum_{m=1}^{N} C(s,m)^*$$
 (6)

where N is the total number of models. As the inter-model diversity of simulated western Pacific precipitation is a major source of uncertainty of projected local SST warming and adjacent ISM circulation changes as explained in the main text, the corrected ISM rainfall changes with observed western Pacific precipitation are constrained to a tighter range with a decrease in the inter-model spread (Fig. 2b), increasing our confidence for ISM projections.

The inter-model uncertainty in projected ISM rainfall change is also significantly correlated with simulating precipitation errors in the tropical southeastern Indian Ocean (SEIO; Fig. 1b). The correlation pattern in the mean precipitation is associated with the inter-model spread in the Indo-Pacific Walker circulation (Supplementary Fig. 8). Alternatively, we build the relationship between the inter-model spreads in projected ISM rainfall change and simulated Walker circulation index by a multi-variant regression analysis as follows:

$$C_{\rm m} = a(P_{\rm m} - kP2_{\rm m}) + b \tag{7}$$

where $C_{\rm m}$ is projected ISM rainfall change for model $m, P_{\rm m} - kP2_{\rm m}$ is simulated precipitation difference between the tropical western Pacific and SEIO (70°–100° E, 8° S–2° N) that represents the Indo-Pacific Walker circulation modulation, and k is the scale factor of precipitation between the western Pacific and SEIO. With a = 0.063, b = 0.057, and k = 0.7, this Walker circulation index correlates with the projected ISM rainfall changes at 0.73 among 24 CMIP5 models (Supplementary Fig. 9), explaining more inter-model spread in ISM rainfall projections (>50%) than the western Pacific precipitation index. The corrected pattern of ISM rainfall projection based on an 'observational constraint' of this Walker circulation index (Supplementary Fig. 9) is very similar to that without including SEIO precipitation biases (Fig. 2d).

Statistical significance. To avoid outlier models dominating the correction results, we also calculate the new corrected climate changes projected by other 23 CGCMs excluding any one selected model. The results excluding any one model are almost the same as those in Fig. 2 from all 24 CGCMs (figure not shown), documenting the robustness of the corrected estimations in this study. To reduce the potential impact of any outliers, we also calculate the Spearman's ranked correlation between the ISM rainfall projections and tropical western Pacific precipitation simulations among 24 CMIP5 models in Fig. 2a. The Spearman's ranked correlation coefficient is 0.68, exceeding the 99.9% significance level. We also use the inter-model standard deviations in assessing statistical significance, since both the uncorrected and corrected ISM rainfall changes among models are approximately normally distributed

Data availability. The CMIP5 and CMIP3 output data are publicly available at http://cmip-pcmdi.llnl.gov. The GPCP precipitation data are publicly available through the web portal (https://www.esrl.noaa.gov/psd/data/gridded/data.gpcp.html). All data used in this study are available online or from the corresponding author on request.

References

- Adler, R. F. et al. The version 2 Global Precipitation Climatology Project (GPCP) monthly precipitation analysis (1979-present). J. Hydrometeorol. 4, 1147–1167 (2003).
- 32. Dai, A. *et al*. The relative roles of upper and lower tropospheric thermal contrasts and tropical influences in driving Asian summer monsoons. *J. Geophys. Res.* **118**, 7024–7045 (2013).
- Sandeep, S. & Ajayamohan, R. S. Poleward shift in Indian summer monsoon low level Jetstream under global warming. *Clim. Dynam.* 45, 337–351 (2015).

- 34. Gent, P. R. et al. The Community Climate System Model version 4. J. Clim. 24, 4973–4991 (2011).
- Hurrell, J., Hack, J., Shea, D., Caron, J. & Rosinski, J. A new sea surface temperature and sea ice boundary data set for the Community Atmosphere Model. J. Clim. 21, 5145–5153 (2008).
- 36. Li, G. & Xie, S. P. Origins of tropical-wide SST biases in CMIP multi-model ensembles. *Geophys. Res. Lett.* 39, L22703 (2012).
- Shiogama, H. et al. Observational constraints indicate risk of drying in the Amazon basin. Nat. Commun. 2, 253 (2011).
- Collins, M. et al. Quantifying future climate change. Nat. Clim. Change 2, 403–409 (2012).
- Bracegirdle, T. J. & Stephenson, D. B. On the robustness of emergent constraints used in multimodel climate change projections of Arctic warming. J. Clim. 26, 669–678 (2013).
- 40. Li, G., Xie, S. P. & Du, Y. A robust but spurious pattern of climate change in model projections over the tropical Indian Ocean. *J. Clim.* **29**, 5589–5608 (2016).